Ismo Väänänen

UHF Power Amplifier Evaluation

Metropolia University of Applied Sciences

Bachelor of Engineering

Electronics

Bachelor’s Thesis

31 May 2023

Abstract

Author:	Ismo Väänänen
Title:	UHF Power Amplifier Evaluation
Number of Pages:	44 pages
Date:	31 May 2023
Degree:	Bachelor of Engineering
Degree Programme:	Electrical and automation engineering
Professional Major:	Electronics
Supervisors:	Teemu Niemi, Hardware Engineer Heikki Valmu, Principal Lecturer

Modern semiconductor products have short lifetimes on the market. This is a problem for industrial equipment with long product lifecycles that can span decades. For that reason obsolescence management is an integral part of electronics design, usually in the form of searching and evaluating new replacement components. This constant search for alternatives and replacements is usually reactive and not proactive. By defining in advance a process for evaluating alternatives, the search can become more proactive.

Such an evaluation process is described in this thesis in the form of a set of acceptance and testing criteria for an ultra high frequency band amplifier meant for operation on the international 860 to 960 MHz UHF RFID frequency range.
A complete amplifier solution suitable for integrating into a product was then designed, prototyped and tested according to the said criteria. Having a proven, integration ready solution at hand allows rapidly reacting to changes in component availability. An additional benefit is the shortened development times for completely new products and new variants of existing ones. This practical aspect of the work also tests the process and criteria themselves.

The prototype amplifier was designed using Altium Designer for schematic capture and layout. QUCS Studio was used for simulations of the initial starting point before finetuning the design to meet the requirements. Testing and performance verification were done at the R&D laboratory of Turck Vilant Systems Oy, for which this work has been produced.

Keywords: testing, UHF, RFID, power amplifier

Tiivistelmä

Tekijä:	Ismo Väänänen
Otsikko:	UHF Tehovahvistimen arviointi
Sivumäärä:	44 sivua
Aika:	31.5.2023
Tutkinto:	Insinööri (AMK)
Tutkinto-ohjelma:	Sähkö- ja automaatiotekniikka
Ammatillinen pääaine:	Elektroniikka
Ohjaajat:	Teemu Niemi, Tuotekehitysinsinööri Heikki Valmu, Yliopettaja

Modernien puolijohteiden saatavuus seuraa markkinoilla olevien tuotteiden elinkaaria. Elinkaarien lyhentyessä ovat komponentit saatavissa markkinoilta entistä lyhyempiä aikoja. Tämä on ongelmallista teollisuuselektroniikassa, missä yksittäisten tuotteiden elinikä markkinoilla voi olla vuosikymmeniä. Vaihtoehtoisten komponenttien etsiminen ja niiden soveltuvuuden arvioiminen ovat integraalinen osa modernia elektroniikkasuunnittelua. Ylensä tämä prosessi on jälkikäteen tapahtuvaa reagointia. Määrittelemällä etukäteen komponenttien valinta- ja testauskriteerit, on prosessia mahdollista muuttaa proaktiivisemmaksi.

Tässä opinnäytetyössä kyseinen määrittely tehtiin lineaariselle tehovahvistimelle joka soveltuu kansainväliselle 860–960 MHz:n UHF RFID -taajuuskaistalle. Vahvistimen suorituskyvylle määriteltiin hyväksyntärajat sekä testit näiden todentamiseksi. Nämä testattiin suunnittelemalla ja toteuttamalla vahvistimen prototyyppi uuden mikropiirin ympärille. Prototyyppi toteutettiin integraatiovalmiina kokonaisuutena, joka on mahdollista kopioida suoraan tuotteeseen minimaalisin muutoksin. Tämä testattu toteutus on siten valmiina, kun edeltävän vahvistimen valmistus loppuu tai kun suunnitellaan kokonaan uusi tuote. Prototyyppivahvistimen vaatimustenmukaisuuden todentaminen myös testaa itse testausprosessin käytännössä.

Prototyypin kytkentäkaavio piirrettiin käyttäen Altium Designer -ohjelmistoa. Kyseisellä ohjelmistolla myös toteutettiin sen piirilevy. Radiotaajuisen osan sovituskomponenttien aloitusarvot simuloitiin käyttäen QUCS Studio -ohjelmistoa. Sovituskomponenttien lopulliset arvot etsittiin perinteisesti vaihtamalla palakomponetteja ja mittaamalla muutos. Vahvistimen mittaus ja testaus suoritettiin Turck Vilant Systems Oy:n tuotekehityslaboratoriossa.

Avainsanat: testaus, UHF, RFID, tehovahvistin, lineaarinen

Contents

List of Abbreviations

LF: Low Frequency. Frequencies between 30 – 300 kHz.

HF: High Frequency. Frequencies between 3 – 30 MHz.

UHF: Ultra High Frequency. The range between 300 – 1000MHz.

RFID: Radio Frequency IDentification

PA: Power Amplifier

EOL: End Of Life. Status for a product for which production has ended.

NRND: Not Recommended for New Designs.

RAIN: RAdio frequency IdentificatioN

1 Introduction

Modern semiconductor lifecycles require the search for alternative parts and solutions to be proactive instead of reactive. We present the evaluation of one potential power amplifier (PA) solution for use in UHF RFID readers. In this thesis we explore the selected amplifier's suitability for such use. In addition to this we layout the basic process and figures of merit for evaluating other power amplifier solutions in the future. We select, prototype and measure one power amplifier solution based on a commercially available Radio Frequency Integrated Circuit (RFIC).

1.1 UHF RFID

As the name states, UHF RFID is a radio frequency identification technology using RF in the UHF range. In the case of EPC Gen2 UHF RFID, the range is from 860 MHz to 960 MHz [1, 17]. This is significantly higher than the 125kHz used in LF tags or 13.56 MHz used in HF RFID tags. Using UHF frequencies instead of LF or HF frequencies makes far field antennas practical. Using far field antennas both at the tag and the reader makes it possible to achieve read ranges on the scale of meters, as opposed to single digit centimeters common with LF and HF RFID tags.
In UHF RFID the most common tag antenna is an electrically shortened variation of the half wave dipole antenna. With the wavelength of the used frequency band being approximately 35 cm, a half wave dipole would be 17.5cm in length. Compare this to the 2400 meter wavelength of 125 kHz and 22meters for 13.56 MHz. On LF the half wave dipole would be 1200meters long! And even the 11meters wide dipole of the 13.56 MHz HF RFID band would be impractical to fit into equipment. Thus LF and HF RFID tags use compact magnetic field antennas where the field strength drops as the cube of the distance, as opposed to the square of the distance for electrical field antennas. Compact antennas inherently make trade-offs in their efficiency to fit the physical limitations of practical products and use cases. While some "long range" HF RFID solutions with up to 2 meter scale read distances do exist on

the market, they are usually large permanently installed systems on the scale of doorways and anti-theft portals [2]. A far cry from a compact handheld reader for convenient inventorying or a forklift capable of reading an entire pallet of goods. UHF RFID makes these use cases practical and compact. Using a higher frequency allows the antennas to be significantly more efficient than their HF or LF counterparts.

1.1.1 Advantages of using UHF

In LF and HF RFID readers the magnetic field antennas in both tags and readers have a tight coupling that makes simple load modulation a feasible way to receive communications from the tag. When it comes to LF/HF RFID tags all communications can essentially be considered nearfield with tight coupling between antennas. With RAIN UHF RFID the tags are usually in the far field. This means that while we get to enjoy the benefits of the field strength only decreasing with the square of the distance and not as the cube of the distance. This means that the achievable read range is much longer with UHF RFID. As the tags need to respond to the reader by re-radiating a signal, the while being powered by the signal from the reader. This means that the power falls with the cube of the distance for UHF RFID and for the magnetically coupled LF or HF RFID it falls to the 9th power of the distance. With passive tags that have no on-board source of power the efficiency of the tag antenna becomes even more important. Along with the output power from the reader illuminating the tag. At long distances the coupling is non-existent, and the tag needs to efficiently capture and then re-radiate the interrogators signal. All of these are easier to achieve on UHF then LF/HF, mostly due to the much shorter wavelength making effective antennas practical.

1.2 Power Amplifier IC

While discrete amplifier solutions made from individual transistors are relatively rare in modern consumer devices due to space and ease of design requirements, they are not unheard of. In telecoms and land mobile radio discrete solutions are still commonly used due to their high output power and flexibility. Recent years has seen highly integrated solutions come to market in the telecoms space and replacing discrete devices in the 10 W to 30 W range in cellular base station power amplifiers. At the same time integrated hybrid amplifiers have essentially disappeared from the land mobile radio space and been replaced by solutions based on discrete transistors. Unfortunately, while advancements in both fields have brought multiple transistors in the 1 W to 5 W range to market, they are often designed and specified for use with 24 V or 48 V supplies in the case of telecoms and 7.4 V or 12 V in the case of land mobile radio. When one considers that the typical UHF RFID reader uses 3.3 V or 5 V supply at the highest, we can see how adapting these solutions to existing products and designs might pose unnecessary hurdles of adding new power supply rails or boost converters.

The rise of the Internet of Things (IoT) market has brought some power amplifier “range extender” solutions targeting the EU 868M MHz band and USA 902 MHz license free bands. Unfortunately, these solutions usually are relatively low power due to regulatory limits on their unlicensed use. A keen observer might notice that the EU 868 MHz band overlaps with ITU Region 2 850 MHz cellular band and USA 902 MHz band overlaps with ITU Region 1 900 MHz cellular band. While this does expand the available amplifier choices, the limitations placed on them due to their use in cell phones makes them unsuitable for UHF RFID. Most cell phones are powered from 3.6V lithium batteries and thus their power amplifier solutions need to operate on those voltages, be compact and efficient. Unfortunately, modern cell phones have very low output powers, in the range of 100-300 mW on most frequency bands and often have extremely integrated multiband solutions. In addition to lower than desired output power, the 850 MHz band cell phone uplink band is 824 – 849 MHz and thus coverage of the 868 MHz band is often not specified or poor. As such most amplifiers targeting cell phone applications are not suitable. The worst aspect of amplifiers targeting cell phones for the industrial electronics designer are the very short product lifetimes. New models and new standards with new bands are released constantly. Not only are the lifetimes short, but the volumes are also large to compensate.

2 Power Amplifier figures of merit

To be able to compare RF power amplifier solutions, some measures comparable between models need to be defined.

2.1 Gain, Power, Bandwidth

Traditionally RF power amplifiers have been evaluated based on their output power, gain, bandwidth, efficiency, and linearity. The exact weighting of each depending on the application. For example, while laterally-diffused metal-oxide transistor (LDMOS) power amplifiers are used in both solid state microwave ovens and cell phone base station radios, the most desirable factors differ. For cooking the lowest cost and highest output power are most desirable. While for base station use in modern multi carrier systems requires extremely high linearity and low distortion, even at the cost of efficiency.

2.2 Efficiency

There are various ways to measure power amplifier efficiency. We are using Power Added Efficiency, or PAE as our metric. This means that the driving RF input power is subtracted from the output power in the efficiency calculation.

2.3 Linearity

Unlike amplifier gain, output power or efficiency, linearity is much harder to define and measure. One common way to measure amplifier linearity is the two-tone test. In it two signals of the same amplitude, but at a frequency offset from each other are introduced to the amplifiers input. Then, depending on the test and standard [example here] under which the test is made, the harmonics and intermodulation products can then be measured. Or the signal levels are increased until a predetermined amount of degradation is achieved, and the levels required for that are noted.

3 Choice of amplifier IC

3.1 Requirements for the new amplifier solution

The new amplifier IC needs to be commercially available with an active status, eg. nothing with EOL or NRND as their status. Reliable availability in volume is key.
In addition to this it needs to function with 3.3V or 5V supply voltage, cover at least 865 MHz to 928 MHz without changing the matching or tuning. Have an output power of at least 1Watt (+30dBm), but preferably 2 to 4Watts (+33 to +36dBm).
All this while being linear enough to amplify low level DSB-ASK or PR-ASK UHF RFID transmission to that output level with low enough intermodulation distortion to still fit the ETSI EN 302 208 V3.3.1 (2020-08) standard spectrum mask [3, 19], and FCC 47 CFR Ch. 1, part 15 [4] regulations for UHF RFID. Usually meeting these two standards means the product also meets the requirements for other markets as well.

3.2 Integrated solutions available on the market

In the previous chapter we defined the figures of merit for RF power amplifiers, now let's look at a selection of alternatives available on the market. These were found by using the parametric search on Digikey.com and Mouser.fi. Not only are these two among the largest distributors, their parametric search for finding parts is particularly good.

Sorting for parts with over +30dBm P1dB, coverage of 865 – 928 MHz, capable of operation with 3.3V or 5V supply voltage and a decent amount of gain. Select components can be seen in Table 1.

Table 1. Selected RF PA IC candidates. Pricing at 100pc in euros. Data gathered from Mouser.fi (2022, 2023), parameters from respective device datasheets.

Part	P1dB	Gain	Supply	Price	Efficiency	Status
SKY65111	+27dBm	39.5dB	2.5 – 5V	2.61	50%	LTB
TQP9107	+30.5dBm	35.5dB	4.3 – 5V	7.56	31%	Active
RF5110G	+32dBm	32dB	2.8 – 3.6V	6.18	57%	LTB
RFPA3800	+36dBm	15dB	5 – 7V	9.57	45%	NRND
GRF5509	+36.4dBm	33.4dB	3 – 5V	3.11	55%	Active
GRF5510	+33.8dBm	29.2dB	3 – 5V	2.47	NA	Active

Even many nominally available chips with good stock and good pricing on distributors might have future availability issues due to being in Last-Time-Buy or NRND. For example, between the initial component selection and the writing of this document the status of Qorvo RF5110G went from Active to Last-Time-Buy [5].

3.3 Why GRF5509?

GRF5509 from Guerrilla-RF promises almost 4W (+36dBm) of saturated power [6], more than the competition, while maintaining high gain and similar price point. While amplifiers are practically never run in saturation, it is still a usable metric for comparing amplifiers. The GRF5509 is in active production and when asked, Guerilla-RF representatives talked about “+10year” typical availability. Another point in its favour is the fact that Guerilla-RF lists UHF RFID as one of its applications and has application notes on the subject. Thus, the product lifecycle might genuinely be very long and not be dictated by the releases of new cellular standards. In addition, the price as whole is competitive with other solutions.

4 Design of the test PCB

4.1 PCB requirements

The expensive and complex stackup was due to the desire to emulate the thermal performance of the amplifier in conditions comparable to the final product. This required the use of a similar PCB stackup with similar laminates. The selected 8-layer stackup (Figure 1) from our supplier uses similar laminates from an internally approved vendor, but the exact stackup is slightly different.

LAYER	NAME OF LAYER	TYPE	THICKNESS mm	VIAS
1	EXTERNAL COPPER	12µm + GalvCu 35µm	0.047	
	PREPREG	1080 (0,063mm)	0.063	
2	INNER FOIL	35µm	0.035	
	INNERLAYER	High Tg 0,2mm 35µm/35µm	0.2	
3	INNER FOIL	35µm	0.035	
	PREPREG	2116 (0,11mm)	0.11	
	PREPREG	2116 (0,11mm)	0.11	
4	INNER FOIL	35µm	0.035	
	INNERLAYER	High Tg 0,2mm 35µm/35µm	0.2	
5	INNER FOIL	35µm	0.035	
	PREPREG	2116 (0,11mm)	0.11	
	PREPREG	2116 (0,11mm)	0.11	
6	INNER FOIL	35µm	0.035	
	INNERLAYER	High Tg 0,2mm 35µm/35µm	0.2	
7	INNER FOIL	35µm	0.035	
	PREPREG	1080 (0,063mm)	0.063	
8	EXTERNAL COPPER	12µm + GalvCu 35µm	0.047	
		THICKNESS (mm) ±10%	1.47	

Figure 1. Used PCB stackup, Copied from Brandner.ee manufacturing quote [7].

This necessitated using different trace widths for impedance-controlled lines. The overall thermal performance should still be relatively close to the design being emulated.

4.2 Practical considerations

The PCB needs to manufacturable and testable. Were it not for our interest in its thermal performance on such a board, we could have used a common 1.6mm thick 4-layer PCB from a low-cost vendor for prototyping. Instead of the current 8-layer design with large of copper planes in the middle layers. While this does noticeably increase the cost of the prototype boards, it also makes our layout and thermal tests more representative of how our design would function in a real-life product.

4.3 Schematic and final layout

We started our design by defining the board stackup to be the same as in a real product. The starting component values for the RF part of the schematic were chosen based on those in the Guerilla-RF provided application note. We added our supporting circuitry for controlling the amplifier and monitoring the PCB temperature. The PCB was sized so that both the matching circuitry and supporting circuitry would fit it comfortably, while having a PCB of convenient to handle size. Despite their inconvenience in manual prototyping, the decision to use 0402 sized surface mount passives in this design was made. This follows larger industry trends and are what end up in actual products. In general passives in 0402 size have better availability due to the high volumes they are used in the industry. As such a design using 0402 sized passives is hopefully more robust against supply chain disruptions than one with 0603 or 0805 sized parts.

4.4 Simulations

In an ideal world both the input and output of the power amplifier IC would have an internal wideband match requiring no tuning and having an excellent return loss across the full band of interest. Unfortunately, this is rarely the case with amplifiers with significant output powers. Usually, one need to apply some external matching circuits at the amplifier output and sometimes also the input.

One traditionally tunes for maximum output power. But without large signal parameters this is not easily possible in simulation software. While those do exist, they are less commonly available for complex devices like these. For our starting point we used gain and output matching as a surrogate for output power. Reasoning that good gain and good input matching should result in good output power. This is partly correct for the GRF5509 and can be confirmed from the public application notes [8] where 4dB of gain is sacrificed to get 2dB more output power. Unfortunately for us, S-Parameters are only available for one bias point. If we adjust the bias point for more output power or more linearity, our simulations become increasingly less accurate and less representative of reality. This means that while we can use the provided S-parameters for things like verifying that our PCB layout or initial matching components result in a functional starting point, the final matching needs to be done with traditional practical methods.

4.4.1 Practical aspects of the simulation

The simulations were done using QUCS Studio [9], a freely available circuit simulation software that works with S-parameters and microstrip circuits. A rough simulation with only ideal components and no microstrips was not too promising, with maximum gain peaking around 700 MHz. Adding in the transmission lines between the passives and the GRF5509 IC brought the maximum gain peak to 824 MHz, as shown in Figure 2 on the red trace. The blue trace shows the simulated input return loss of the amplifier.

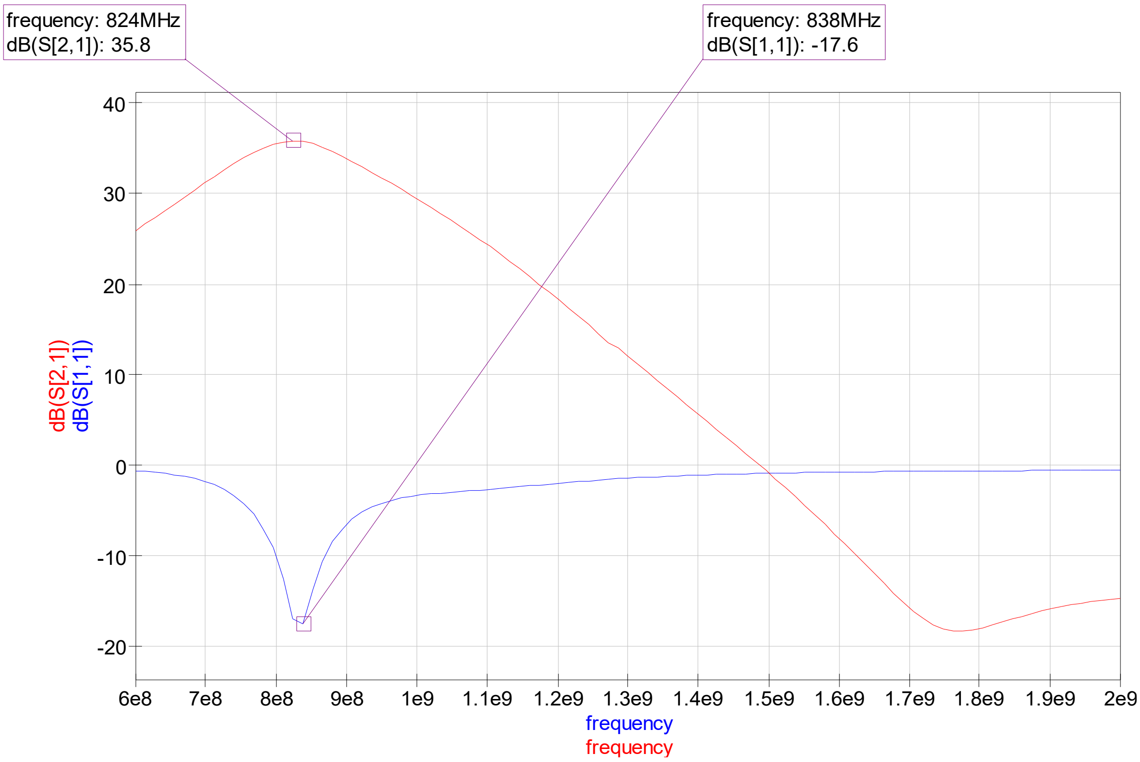

Figure 2. Simulation results of the initial schematic with PCB effects included.

Grounded Coplanar Waveguide (GCPW) 50Ω transmission lines were used between the input connectors, passives and the GRF5509 IC. While the test PCB designed here could have accommodated traditional microstrip transmission lines, the final application could not. Using GCPW allows for a much tighter layout with less coupling and radiation to and from the RF traces. Our used stackup (Figure 1) has 63µm type 1080 prepreg between top and second layer. This results in extremely narrow traces when GCPW ground plane is directly beneath the top layer on layer 2. Adding a cut out in layer 2 ground plane and instead using layer 3 as our ground plane increased the distance from nominal 63µm to nominal 298µm. This accordingly increases the width of our 50Ω lines from 100µm to 425µm. Not only is this more robust against manufacturing tolerances, it also has less loss and is a good mechanical fit to nominally 500µm wide 0402 (imperial) sized SMD passive components. QUCS Studio does not seem to easily support multiple PCB layers, so separate PCB substrates were defined for the 100µm wide and 425µm wide GCPW lines (Figure 3). Inconveniently, the effective permittivity (ε_r) of the Panasonic R-1650V type 1080 prepreg was 4.0 on 1 GHz and for the

Panasonic R-1755V core was 4.5 [10, 3-4]. As the prepreg layer was only 63µm thick, we used 4.5 ε_r for both in the thicker substrate model.

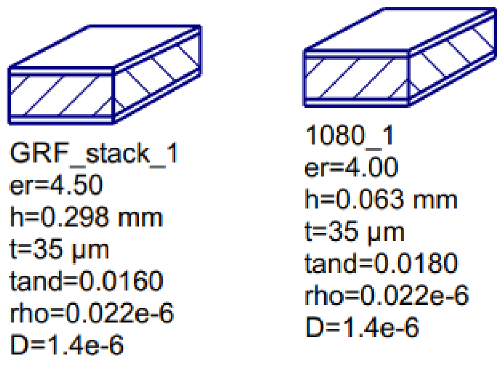

Figure 3. PCB substrate parameters used in simulations.

Manually adding custom PCB substrate materials to QUCS Studio was not particularly well documented, but straightforward and easy to do. All that was required was adding the new substrate definitions to the human readable substrate definition file with a text editor.

4.4.2 Developing the power amplifier IC match

For optimum output power, gain, linearity, and efficiency the GRF5509 needs some additional input and output matching circuits. We used the input matching from the Guerilla-RF application note “GRF5509 865-928 MHz: Linear Tune vs. High Power Tune” [8] as our initial starting point. After the boards were manufactured, assembled and measured, the exact input matching circuit was developed. As the input impedance of the device depends on the output match, output power level and the bias points of the internal amplifier stages, the final matching circuit depends on the final bias point.

In addition to custom tunes available on Guerilla-RF.com [11] we also received additional information on UHF RFID specific matching circuits from the Guerilla-RF applications engineering team via email. Included were also some S-parameter files, but those are mostly only useful for developing the input match and not the large signal output matching circuit. Using the provided S-parameters allowed us to design the initial matching circuit for our board and more importantly it allowed us to verify that our simulation at least somewhat corresponded with reality. The resulting simulated input and output matching can be seen in Figure 4.

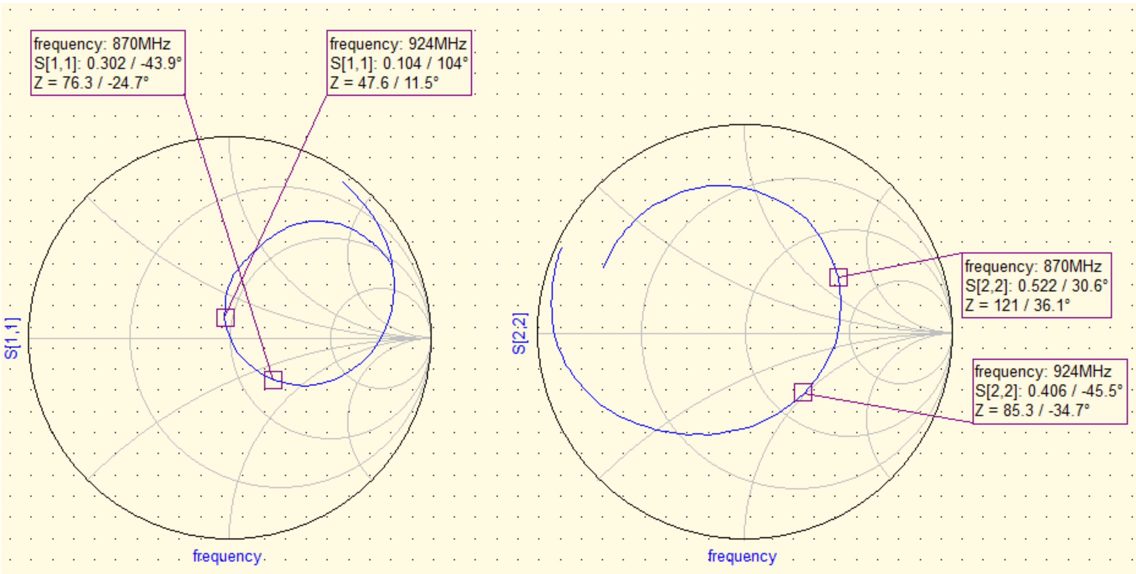

Figure 4. Simulated input and output matching after fine tuning.

Finetuning the simulation to match more closely what we measured later helped make finetuning the design easier. Developing the matching circuit would have been easier, had we not had to change the bias point to a less linear one from the initial one to get more output power.

4.4.3 Practical RF Matching

The simulations were remarkably close to the measured performance of the test board with component values from the initial schematic. Unfortunately, the simulated input matching starts differing from reality when the bias point is changed. As the amplifier biasing affects the output impedance and thus the impedance seen at the input.

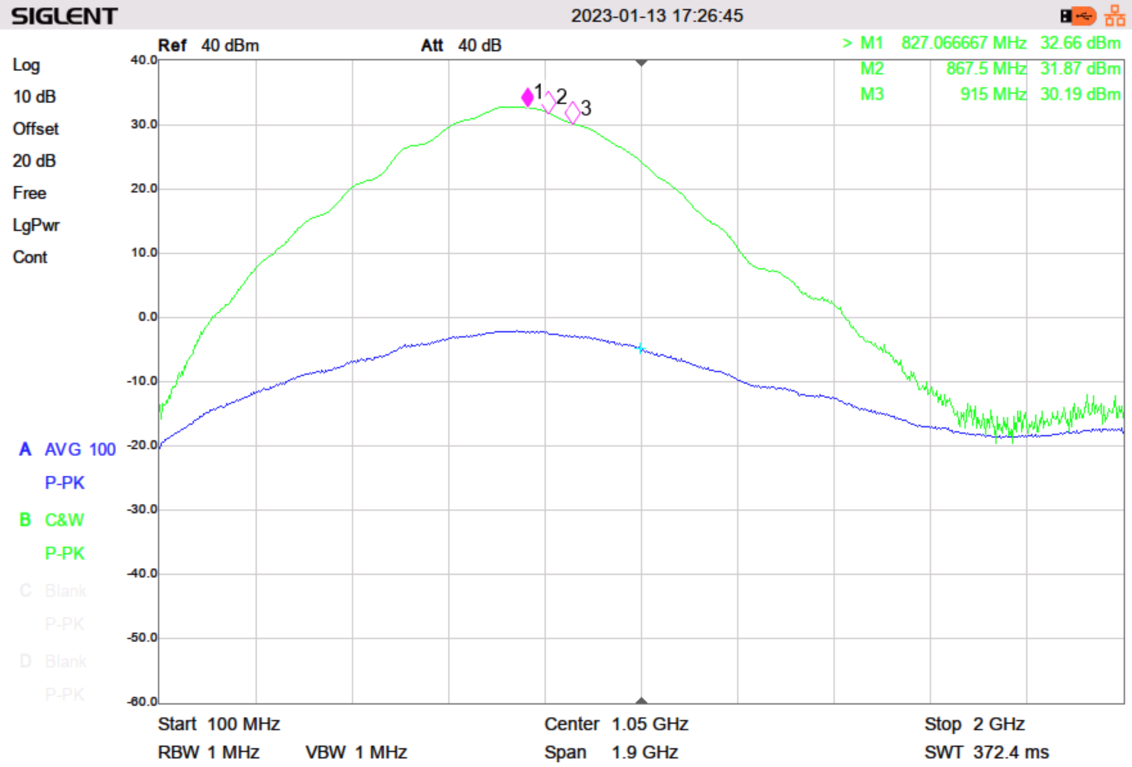

Figure 5. Output power from initial prototype.

As stated in 4.4, with GRF5509 one can essentially trade gain and linearity for more output power. To do that the bias point needs to be changed. And when the bias point is changed, the output and input impedances change. This makes simulations less helpful and forces us back to swapping capacitors and then measuring the results. Unless one has access to a two-port vector network analyser and stub tuners for doing a load-pull to discover the optimum output impedance in those operating conditions. Unfortunately, these are not common pieces of equipment in smaller R&D laboratories. This was also the case here. With the traditional methods we were able to get up to +34.7 dBm, or 2.9 W saturated output power on 867.5 MHz. This took a significant amount of time due to the cycles of manually swapping parts in the matching circuitry and measuring the change in performance.

The initial bias point was slightly adapted from the application note to use more easily available standard resistors. As such the 1160 ohm resistor was replaced by 1200 ohms and the 3570 ohm resistor was replaced by 3600 ohms. Both are deliberately larger values that move the bias point to a very slightly less linear one. Later, when tuning the amplifier, bias resistors were changed to significantly larger values to get more output power. The values in the current design are 3300 ohms for R2, setting the first stage bias current. And 6800 ohms for R1, setting the second stage bias current. This gave more power, but not as much as hoped. Largest increase in the RF output power was realized when analysing the power delivery network for voltage drops. When directly measured at the amplifier input terminal, the supply voltage was only 4.3 volts. First change in the DC supply path was replacing the 24 µH DC bias choke with a physically larger one rated for higher currents. This did increase the power somewhat and raised the voltage seen after the choke to 4.7 volts. It was determined that the 2.54 mm pin header and the 1mm wide trace were insufficient for the approximately one and a half ampere of supply current the amplifier pulls at maximum output power. After it was determined that both 2.54 mm plugs and alligator clips had too much resistance, a 1.5 mm² DC supply cable was soldered directly to the board. With power wired directly to decoupling capacitor C5 and bypassing the inline zero-ohm resistor R3 a gain of almost 1 watt in output power was measured on 867.5 MHz. In Figure 6 one prototype amplifier with its distinctive towers of stacked capacitors and hardwired DC supply cable can be seen. Due to the increased series inductance stacking capacitors of smaller value on top of the one already installed on the board is not a perfect method for developing impedance matching networks. Doing so makes rapid iteration possible and allows for smaller steps in capacitance than what stocked capacitor values would otherwise allow. Due to UHF RFID operating below 1 GHz, it was possible to utilise less than perfect methods like these.

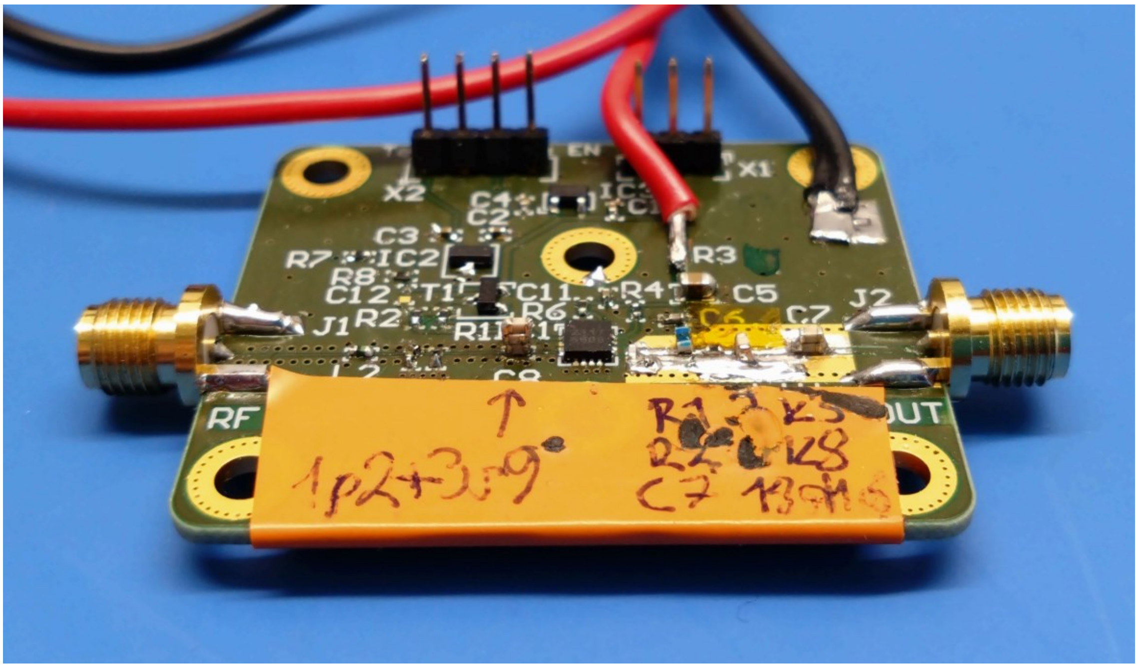

Figure 6. One amplifier prototype in the middle of tuning.

In hindsight, the RF input trace to the amplifier should have used the same trace width as the output one. Not only was it a perfect mechanical fit to 0402 sized passive components used to implement the matching. The wider trace also accommodates 0603 sized components better.

4.4.4 Implementing the supporting circuitry

It should be possible to monitor the temperature of the amplifier board and to disable its RF output without disconnecting the supply voltage to the board. Board temperature is monitored with a Texas Instruments LM60CIM3 temperature sensor. As we wanted to isolate the LM60CIM3 from potential noise on the 5V supply rail, we employ a low cost 3.3V low drop out regulator (LDO) in SOT-23 case on board to generate a clean 3.3V rail from the main 5V supply. Many other noise filtering solutions could have also been used here as the quiescent current of LM60CIM3 is less than 110μA. Typical UHF RFID data rates are between 40 and 640 kHz. As the modulation used is amplitude shift keying (ASK), the modulated data is strongly superimposed on the power amplifier supply rail. Using LC or RC filters to supress this noise on the power supply would require inconveniently large components to realise adequate noise rejection. The active feedback loop in even low-cost voltage regulators excels at rejecting low frequency noise. In the case of LM3480IM3-3.3 the power supply rejection ratio (PSRR) is at least 40dB from 10 Hz to 1 MHz with a 100 nF output capacitor [12, 9].

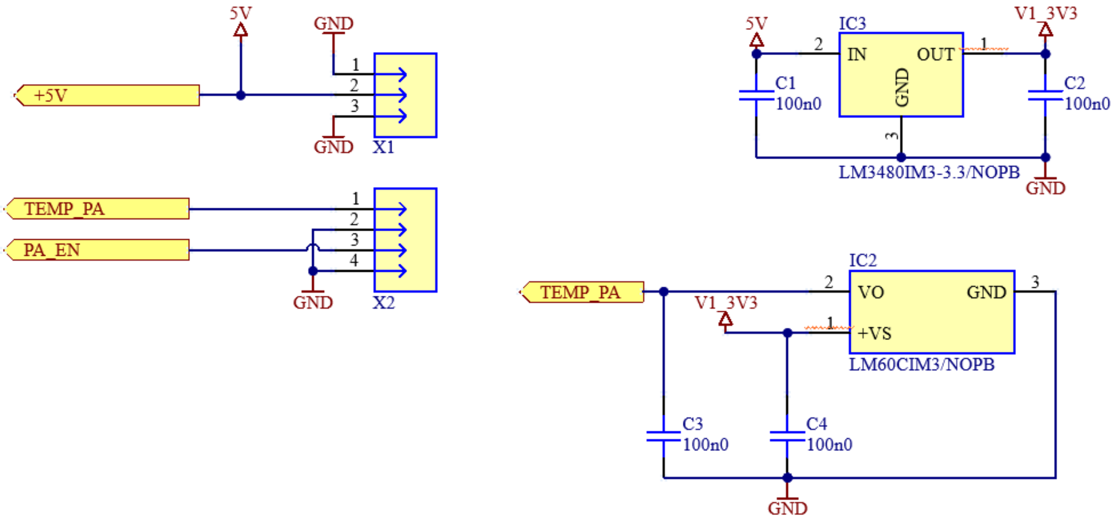

Figure 7. 3.3V regulator, DC connection and temperature monitoring schematic.

While the schematic in Figure 7 shows an LM3480UM3-3.3/NOPB as the regulator for 3.3V rail, the part actually used ended up being TS3480CX33, a drop-in pin compatible alternative from Taiwan Semiconductor due to the Texas Instruments LM3480 not being available at assembly time.

The amplifier RF output is controlled via the bias pins “VEN1” and “VEN2”. These respectively set the bias point for the first and second amplifier stages. Logic level control of these signals is achieved with a BSS84 P-channel MOSFET installed in line with the bias supply. As high-side switching was required, a simple P-FET was used here. The BSS84 was chosen based on it being compatible with both 3.3V and 5V logic level signals. It’s good availability and low price also contributed to it being chosen. Additional robustness towards mistakes is afforded by the high Gate-Source voltage of ±20 volts. This means the transistor will survive both too high and wrong polarity control voltages. The resistance from drain to source (RDS(on)) of BSS84 is 1 to 2.5Ω for 3.3 to 5V across 25°C to 125°C, as shown in Figure 8 [13]. This is conveniently low compared to the kilo-ohm range bias resistors and practically eliminates the BSS84 as a source of drift for the amplifier bias point with temperature.

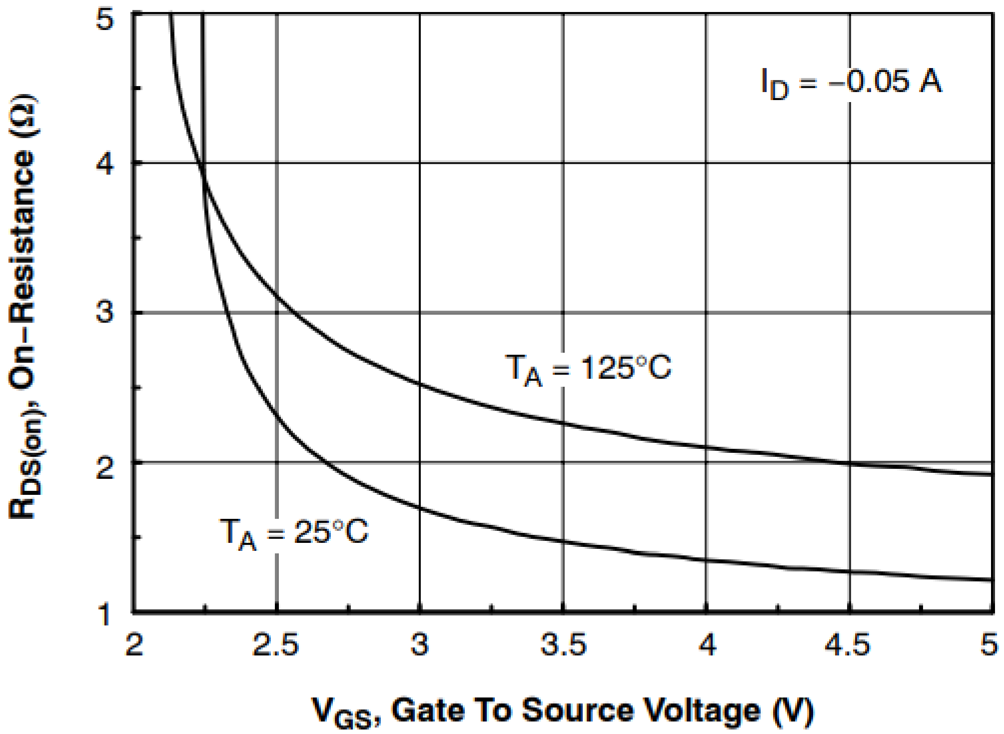

Figure 8. BSS84 On-Resistance Variation with Gate-to-Source voltage. Copied from onsemi BSS84 datasheet [13].

To ensure a known state with floating enable input, the BSS84 gate was pulled down to ground via a 10kΩ resistor. This results in the amplifier turning on when no control signal is present. This made testing more convenient, in a practical application the gate should be pulled high to ensure that the amplifier defaults to a safe state. The 33pF shunt capacitor in parallel with it was included as a high frequency noise filter. This capacitor forms an RC low pass filter in conjunction with the 1kΩ gate series resistor with the approximate corner frequency of 4.7 MHz. This is suitable for rejecting high frequency RF noise that might couple into the control lines during testing. The exact capacitor value is less important, due to the BSS84 typical input capacitance of 73pF dominating with these small values. If on some later date it is determined that coupled RF energy or transients are causing trouble with the enable circuitry, the capacitor can be increased, as long as the introduced delay stays manageable.

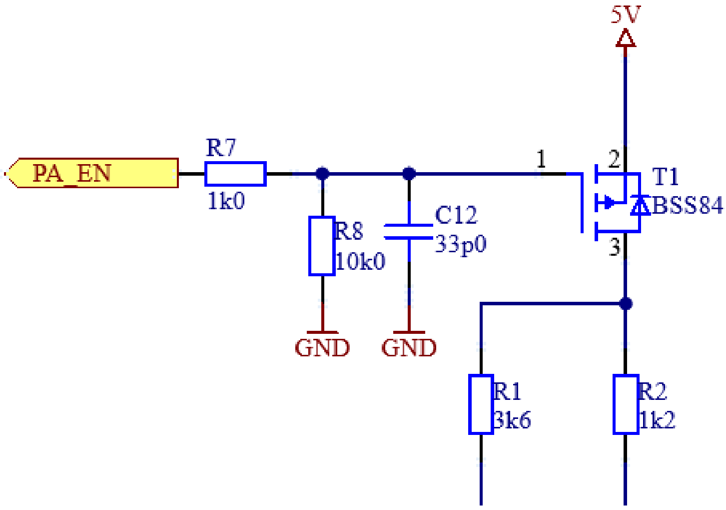

Figure 9. Amplifier control circuit.

Initial values for bias resistors R1 and R2 are shown here in Figure 9. These values were adapted from the Guerilla-RF application note “Linear tune vs. High power tune” [8].

5 Testing and testing methodology

Before any measurements or testing can be performed

5.1 Defining Pass-Fail criteria for the amplifier

To be able to test if our new solution meets our requirements, we need to spell out the Pass-Fail criteria and exact limits we want to be able to reach with the final revision of the amplifier.

5.1.1 Test suite

The following suite of tests and testing criteria was developed for evaluating the amplifier.

5.1.2 Gain

At least 30dB of gain is desired. This should allow us to reach full output power with +3dBm of drive. Large signal gain below 27dB can be considered a fail. The maximum output of the tracking generator in Siglent SSA3032X is 0dBm [14, 6]. A small buffer amplifier might be needed in some cases to measure the proper saturated power.

5.1.3 Output power

Output power of at least +33dBm (2W) was desired. But the aim is to achieve at least +35dBm (4W). We will measure the output power on the spot frequency according to ETSI EN 302 208 V3.3.1 (2020-08). This means setting the spectrum analyser to 1kHz Resolution Bandwidth (RBW), using the same width for Video Bandwidth (VBW) as for RBW, in a 1 MHz span on our centre frequency. The detector mode is set to average and trace to max hold.

5.1.4 Power Added Efficiency

While there are many ways to measure power amplifier efficiency, we are using Power Added Efficiency “PAE” (1) as our figure of merit.

$$PAE = \frac{P_o - P_{drive}}{P_{in}} \tag{1}$$

Where P_o is the RF output power, P_{in} the DC input power into the power amplifier and P_{drive} the RF power we feed to the input port of the amplifier. This means we subtract the drive power from the output power used to calculate the amplifiers efficiency. We hope to achieve PAE in the 50-60% range. We will consider PAE below 40% a fail.

5.1.5 Thermals

In industrial use the ambient temperature can reach +60°C. As such the IC package temperature needs to stay below +85°C. This should ensure chip junction never reaches the specified absolute limit of 170°C. This ties into PAE and achieving the desired output power within these limits.

5.1.6 Linearity

Not only are high output powers at great efficiency desired, it should also be decently linear at that power level. Many of the evaluated solutions were marketed towards the telecom sector and thus the strict linearity requirements that come with wide LTE signals and transmitting multiple wide carriers.
UHF RFID is much narrower, and the modulations used are far less complex. However, our amplifier still needs to be linear to ensure spectral purity. Higher linearity helps us fit the ETSI emissions spectrum masks at high powers. This is due to decreased intermodulation between the carrier and modulated sidebands. As shown in Figure 10, on the ETSI low band of 865 MHz to 868 MHz UHF RFID band the ETSI EN 302 208 V3.3.1 (2020-08) standard [3, 19-20] does not specify a relative power level (eg. dBc) for emissions outside the spectrum mask. Instead, absolute limits in dBm are specified, +3dBm at +-100kHz offset, -36dBm at 200kHz offset and -46dB at +-400kHz offset from the channel centre frequency.

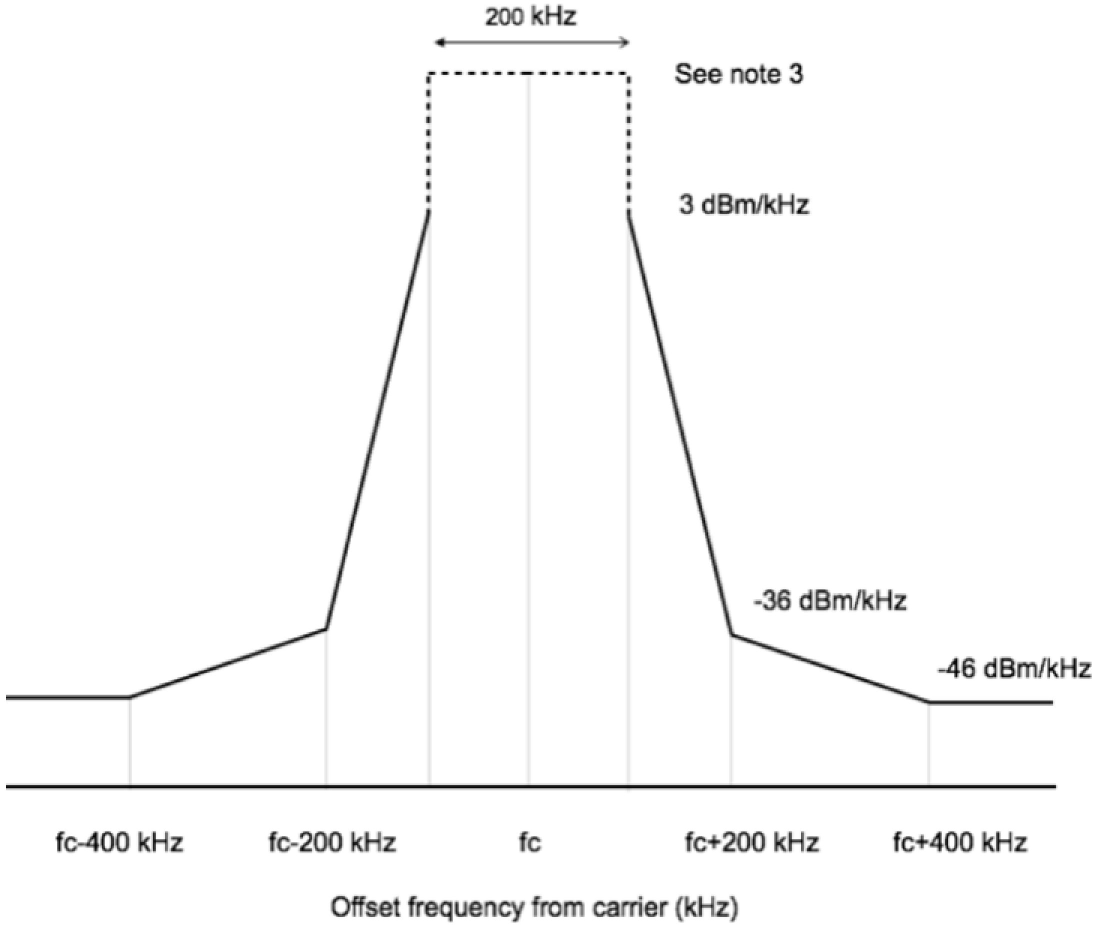

Figure 10. Limits for lower ETSI band. Copied from ETSI EN 302 208 V3.3.1 [3]

On the ETSI upper band of 915MHz to 921MHz the limits are less strict at +6dBm at +-200kHz offset, -36dBm at 400kHz offset and -46dBm at +-800kHz offset from the channel centre frequency, as shown in Figure 11.

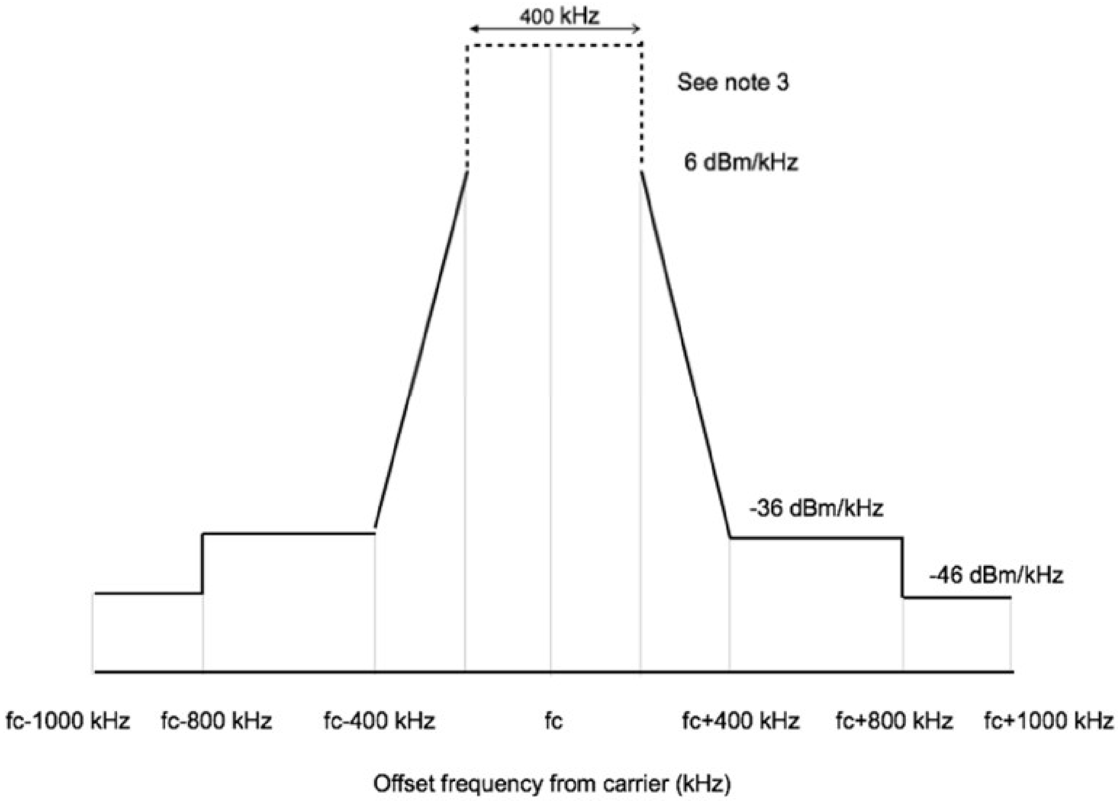

Figure 11. Limits for ETSI upper band. Copied from ETSI EN 302 208 V3.3.1 [3]

Based on this the amplifier OIP3 is measured on both ETSI and USA band with standard dual tone test. With a 200 kHz separation between the tones.

5.1.7 Input matching

To transfer maximum power into the amplifier, it needs a decent input match. As driving power to it is easier when it does not get reflected. Filters preceding the power amplifier also require 50ohms termination to realize the specified passband and insertion loss. Thus, it is desirable to achieve at least 6dB return loss at the amplifier input port. While it is not a major concern here, the matching at the amplifier ports does affect its stability.

5.1.8 Regulatory limits

We want our harmonic emissions and in-band spurious emissions to meet or exceed the ETSI 302 208, FCC and ISO 18046 requirements. Especially we want to fit the emissions spectrum mask. This ties into the question of linearity and maximum achievable output power while meeting regulatory limits set in ETSI EN 302 208 V3.3.1 (2020-08) [3]. As final products are complete systems with additional filtering, it is not possible to completely evaluate the amplifiers contribution to overall regulatory compliance.

5.2 Test setup

The amplifier was tested at the R&D laboratory of Turck Vilant Systems Oy (TVS) with available equipment in the following setups.

5.2.1 Gain

Amplifier gain was measured using the tracking generator equipped Siglent SSA3032X spectrum analyser at TVS and with a Tekbox 20 dB 10 W attenuator in series with the input. As the amplifier should have over 30 dB gain and +30 dBm output power, the attenuator was required between the amplifier output and the spectrum analyser input to protect it from damage. Overdriving the spectrum analyser input to distortion will generate spurious responses that do not exist in the output signal. While this does not damage the instrument, such distortion will make the amplifier look worse than it is. An additional attenuator was also used at the amplifier input to ensure that both the tracking generator and amplifier see a good 50ohm match. The tracking generator output in Siglent SSA3032X can be adjusted down to -20dBm, which should not overdrive the amplifier in any situation [14, 6]. Prior to the measurement, connecting cables are calibrated out. While the loss in the cables made from RG-223 cable should be negligible on 860 – 960 MHz, it is good practice to do so to ensure the most accurate measurement.

5.2.2 Output power

Output power is measured with the Siglent SSA3032X at TVS and with a Tekbox 20 dB 10 W attenuator at spectrum analyser input. This ensures that the spectrum analyser input is not damaged nor is it driven into distortion. We'll use the channel power measurement utility in the Siglent SSA3032X to measure the power we get at a 1MHz wide channel on ETSI lower band and 2 MHz for ETSI upper band. FCC testing is also done according to Part 15. Like previously done in the gain measurement, cables will also be calibrated out.

5.2.3 Power Added Efficiency

As we known the drive power, we only need to measure the DC input to the power amplifier side of the test board, this is easily done using the 0ohm jumpers fitted for this purpose. On the drive power we trust the factory calibration in our Siglent SSA3032X spectrum analyser. We use the Siglent to measure both the driving power and the output from the amplifier. This ensures that both numbers are comparable. The overall contribution of the drive power is small in this case, but subtracting it is good practice when evaluating amplifier efficiency. While we could simply trust the displays on our laboratory power supply, we can get better accuracy and if desired, easier logging on computer with our Agilent 34410A 6½ digit multimeter.

5.2.4 Thermal performance

The Agilent 34410A multimeter supports PT100 and PT1000 RTD's and select thermistors.
A low thermal mass PT1000 RTD is affixed on top of the amplifier IC chip to monitor the case temperature. PCB temperature is monitored with the onboard LM60CIM3 temperature sensor wired to a separate multimeter. As there can be differences in efficiency between 867 MHz and 915 MHz test frequencies, we'll test on both at the output power levels of +30 dBm, +33 dBm and saturated.

5.2.5 Linearity

We want to measure the third order intercept point or OIP3 of the amplifier. Using OIP3 to represent amplifier linearity is a well-established method in the industry, resulting in numbers easily compared across devices and manufacturers.
We shall measure OIP3 on the following frequencies with a 5 volt supply voltage on 867, 902 and 928 MHz centre frequencies, with the tones spaced 100 kHz above and below the centre frequency.

5.2.6 Input matching

The input matching will be measured with a NanoVNA V2 unit. Accuracy of a low-cost instrument like NanoVNA V2 is acceptable and repeatable on frequencies below 1 GHz. Likewise, the calibration kit supplied with it works very well at these low frequencies, giving us accurate, repeatable performance. An additional, larger 1001 point calibration can be done with the instrument connected to a PC. This is particularly useful when measuring the matching across a wider band.

5.2.7 Regulatory limits

Our main regulatory compliance interest is having our eventual UHF RFID readers emission fit the ETSI spectrum mask. Thus, linearity and intermodulation distortion addressed in output power and linearity do cover it. Harmonic output is reduced below the required limits by a separate low pass filter. Decent linearity should be doable with the power amplifier, as we will not be running it in saturation or too close to it. This should also reduce harmonic generation.

6 Test results

Initial and final measurements.

The initial prototype was measured to establish a reference starting point for component values and performance. Full set of measurements as defined in chapter 5 were not fully performed, as the initial prototype was off frequency. The final iteration was then fully measured and evaluated.

6.1 Initial results

Upon measuring the amplifier for the first time we discovered that our tune was low, with maximum gain (Figure 12) and maximum output power (Figure 13) being centred on approximately 827 MHz, over 40 MHz below the preferred point in between ETSI and USA bands. Nevertheless, the results were very promising as we had 36dB gain on 827 MHz, 34.5dB gain on 865.7 MHz and 32.5dB gain on 915MHz.

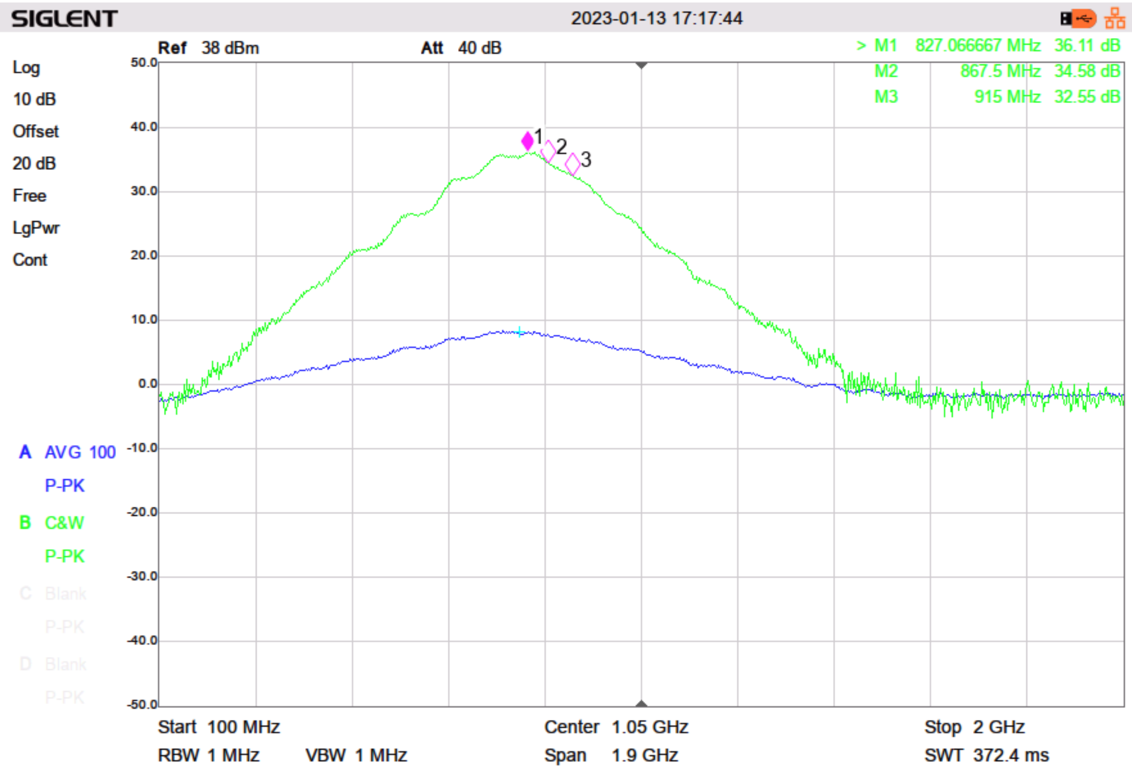

Figure 12. Amplifier small signal gain between 100 - 2000 MHz, with -20 dBm drive. The green trace shows the amplifier gain.

While falling short of at least +33 dBm across the band, the amplifier had significant gain. It was a very good starting point for fine tuning the design. The wavy, stepped response was also observed with a straight through cable between the tracking generator output and spectrum analyser input. This behaviour was determined to be an artefact of the tracking generator implementation in the Siglent SSA3032X spectrum analyser. Next, the output power was increased from the lower limit of -20 dBm to 0 dBm, to drive the amplifier into saturation across the frequencies of interest.

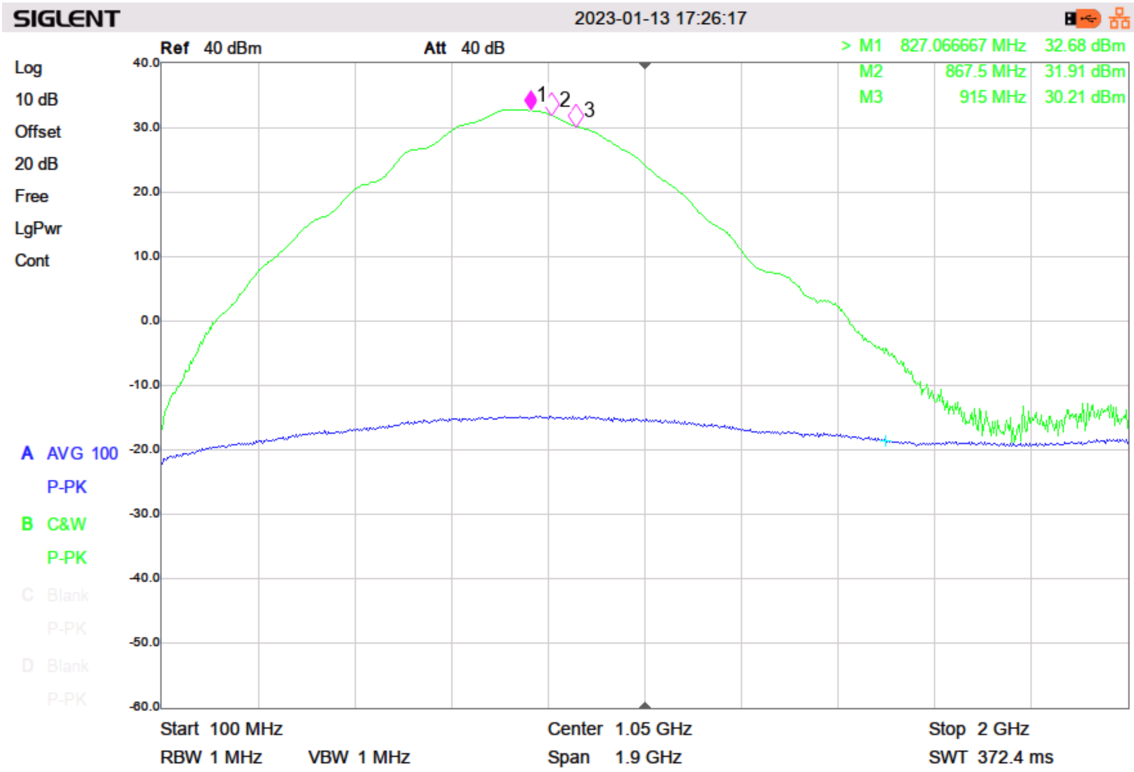

Figure 13. Amplifier output power between 100 - 2000 MHz, with 0dBm drive. The green trace shows output power in dBm. The blue trace has averaging turned on and can be safely ignored.

The initial output power starting point was +32.6dBm on 827 MHz, +31.8 dBm on 867.5 MHz and +30 dBm on 915 MHz. These were below the target output power, but having almost two watts on the lower frequency showed that proper +33 dBm was achievable, with some additional tuning. With the amplifier in or near saturation, the response also smoothed out.

Table 2. Amplifier performance starting point.

Test Frequency	Gain (dB)	Maximum output (dBm)
867 MHz	34.58	31.87
915 MHz	32.55	30.19

The measured amplifier gain and output power on the two test frequencies are in Table 2.

6.1.1 Measured Gains

Both small signal gain and power gain were measured from the prototype amplifier. The results are documented in Table 2, with Figure 12 and Figure 13 showing the measurement across the 100 MHz to 2000 MHz span. Small signal gain was measured with the tracking generator set to -20dBm output power. For the large signal gain measurement, the tracking generator was set to 0dBm.

For the initial quick tests 867 MHz was used as the test frequency for the EU band and 915 MHz for the USA band. 915 MHz conveniently sits in the middle of the USA band and is also near the Chinese band. This makes it a good surrogate for overall performance. Expanding on it, the amplifier was also measured at the spot frequencies of 867, 902, 923 and 928 MHz.

6.1.2 Output power

Initial output power tests were done using the 0dBm maximum drive power setting available from the tracking generator. In later tests it was discovered that the 0dBm drive was insufficient to properly saturate the amplifier in some situations. This was mitigated by quickly fabricating a buffer amplifier from available surplus. A surplus board with an MSA-0385 MMIC from Hewlett-Packard was chosen due to its moderate gain of 12 dB at one gigahertz and

+10 dBm P1dB at the same frequency. This makes it a good fit for GRF5509's absolute maximum input power for of +13 dBm. A 3 dB connectorized attenuator was added in between the buffer amplifier and the GRF5509 board. This further limited the gain and output power of the buffer to such level that damage was not possible with the +0 dBm drive power available from the Siglent SSA3032X. The attenuator further ensured that both amplifiers would see at least 6 dB return loss on all frequencies of operation.

6.1.3 Thermal performance

Thermal testing was limited due to time and equipment. The setup used for thermal testing is shown in Figure 14. Due to no environmental cabinet being available, the testing was conducted in open air with long integration times.

Table 3. Thermal performance of the initial version.

Test Frequency	Power (dBm)	Chip case (°C)	Ambient (°C)
867 MHz	+30	+52.7	+21.4
915 MHz	+30	+53.1	+21.4

Thermal testing was limited due to time and equipment. The setup used for thermal testing is shown in Figure 14. Due to no environmental cabinet being available, the testing was conducted in open air with long integration times. As seen in Table 3, the chip case temperature staid well below the +85°C limit specified in the GRF5509 datasheet [6, 4].

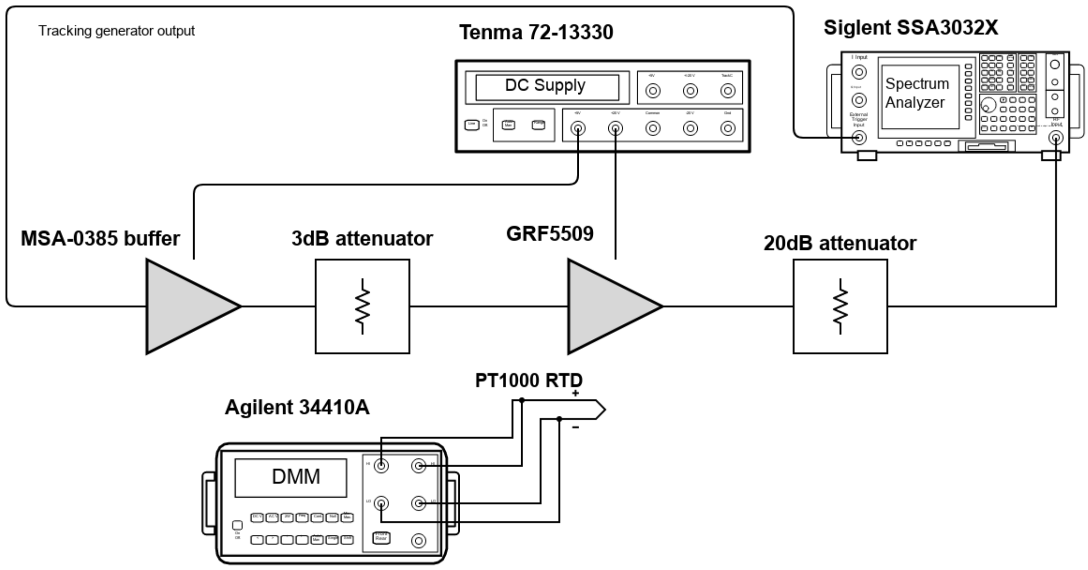

Figure 14. Setup used during thermal testing.

Chip temperature was monitored with a PT1000 RTD connected to our Agilent 34410A multimeter via four wire measurement. The model NB-PTCO-154 low thermal mass PT1000 type RTD from TE Connectivity was affixed on top of the 7 mm x 7 mm QFN case of the GRF5509 with Fischer Elektronik WLFT 404 adhesive thermal film [15, 5; 16]. The ambient temperature during tests was 21.4°C.
It is acknowledged that thermal performance results obtained this way are at most suitable for indication only. These measurements do indicate that it is possible to adequately heatsink and cool the GRF5509 running at maximum output power with a 100% duty cycle for extended periods.

We did not evaluate the linearity of the initial starting point tune of the amplifier.

6.1.4 Input matching

The matching at the input was measured with a NanoVNA V2 low-cost network analyser across 600 MHz to 1000 MHz span. Hard copies were saved by connecting the VNA to a computer running the vna-qt [17] software. Using vna-qt allowed us to have a 1001-point calibration, trace averaging, better hardcopies and allowed us to save the measurements as Touchstone S-parameter files for later analysis.

Table 4. Input return loss of the initial prototype.

Frequency (MHz)	Input return loss (dB)
867.5	8.5
902	7.9
923	7.6
928	7.5

Precise values for the measured return loss on test frequencies is presented in Table 4, for comparison against performance measured later.

6.2 Final version performance

The final version of the amplifier was measured more extensively than the initial prototype.

6.2.1 Gain and output power measurement

We are using 867.5 MHz as the test frequency for the EU band and three points across the 900 MHz band. Using 902, 923 and 928 MHz gives us the performance at the edges of the USA FCC band and one in the middle of the Chinese band.

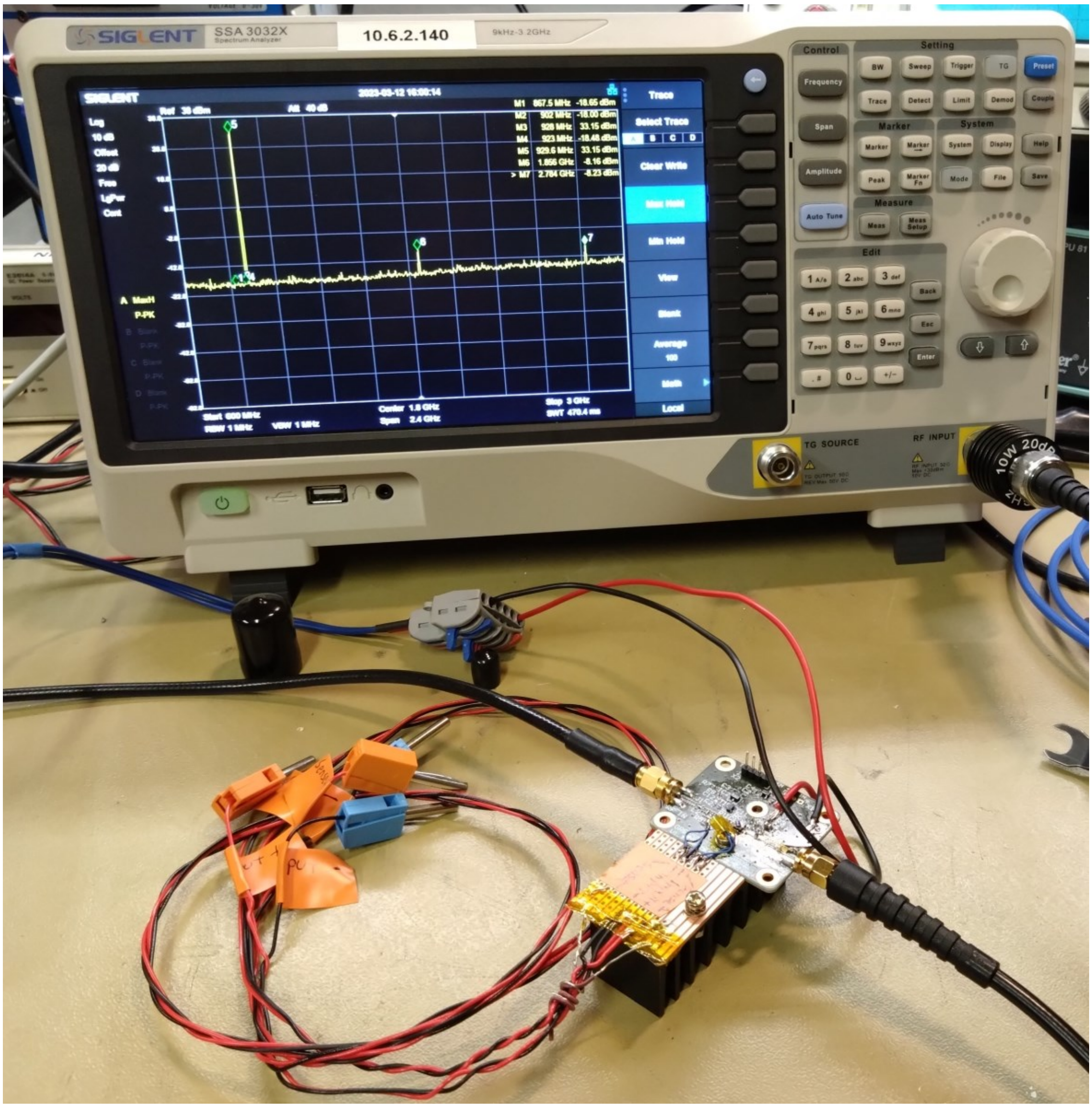

Figure 15. Amplifier harmonics measurement in progress.

With the 20 dB attenuator inline and internal attenuator set to 20 dB, there was no danger of the Siglent SSA3032X frontend distorting and skewing test results.

Table 5. Output power with nominal 0 dBm drive power.

Test Frequency	Output (dBm)	Drive power (dBm)	Power gain (dB)
867.5 MHz	31.12	-0.96	32.08
902 MHz	30.82	-0.86	31.68
923 MHz	29.99	-0.82	30.81
928 MHz	30.05	-0.87	30.92

Full one watt of RF output power was achieved with less than 0 dBm of drive. This meets the requirements specified in section 5.1.2 with dynamic range left over to account for unit-to-unit variability.

Table 6. Output power with nominal +6 dBm drive power.

Test Frequency	Output (dBm)	Drive power (dBm)	Power gain (dB)
867.5 MHz	34.22	+4.66	29.56
902 MHz	33.73	+5.1	28.63
923 MHz	33.23	+5.2	28.03
928 MHz	33.17	+5.23	27.97

With approximately +5 dBm of drive, the output power was above two watts on all test frequencies. As the amplifier saturated like expected, the measured power gain was lower than with +0 dBm drive.

Table 7. Harmonic suppression with nominal +30 dBm output power.

Test Frequency	Fundamental (dBm)	2nd harmonic (dBc)	3rd Harmonic (dBc)
867.5 MHz	+30.97	-40.45	-36.84
902 MHz	+30.58	-41.23	-38.99
923 MHz	+29.74	-39.41	-41.27
928 MHz	+29.77	-39.22	-42.18

Harmonic suppression was good for a single ended amplifier at the nominal one Watt output level setting.

Table 8. Harmonic suppression with the amplifier saturated.

Test Frequency	Fundamental (dBm)	2nd harmonic (dBc)	3rd Harmonic (dBc)
867.5 MHz	+34.18	-40.22	-31.09
902 MHz	+33.70	-	-
923 MHz	+33.23	-40.90	-39.53
928 MHz	+33.15	-41.31	-41.11

OIP3 was measured by combining two signal generators with a Mini-Circuits ZX10-2-12-S+ 2 - 1200 MHz splitter and then connecting the common port to the amplifier input directly. The port 1 to port 2 isolation is 20.62dB according to the ZX10-2-12-S+ datasheet [18]. This should ensure that the signal generators are not coupling to each other's outputs in significant amounts. This is relevant with some signal generators that have their wideband output power levelling detector after the internal attenuators and variable gain amplifiers. This type is susceptible to give erroneous output levels if RF energy is present on their output port, even if it is on a different frequency. The Agilent N5182A and Anritsu MG3670B are not susceptible to this. During the measurement the output power between tones was observed and adjusted to be at the same level.

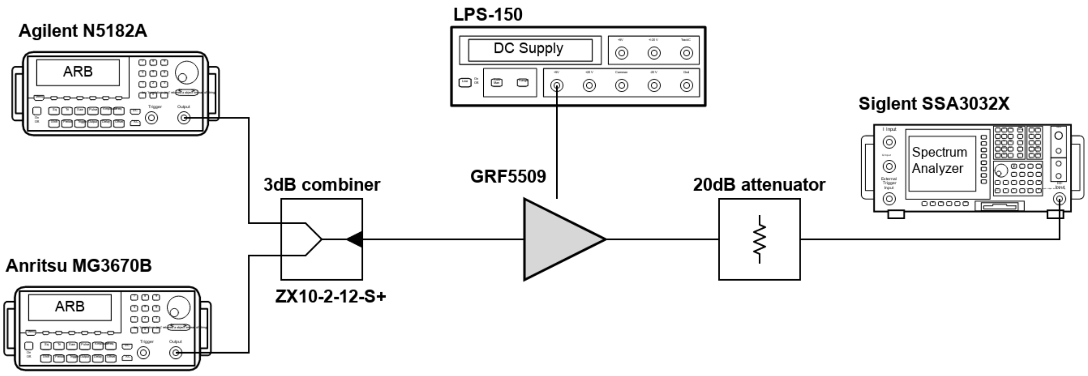

Figure 16. Wiring of the two tone OIP3 measurement.

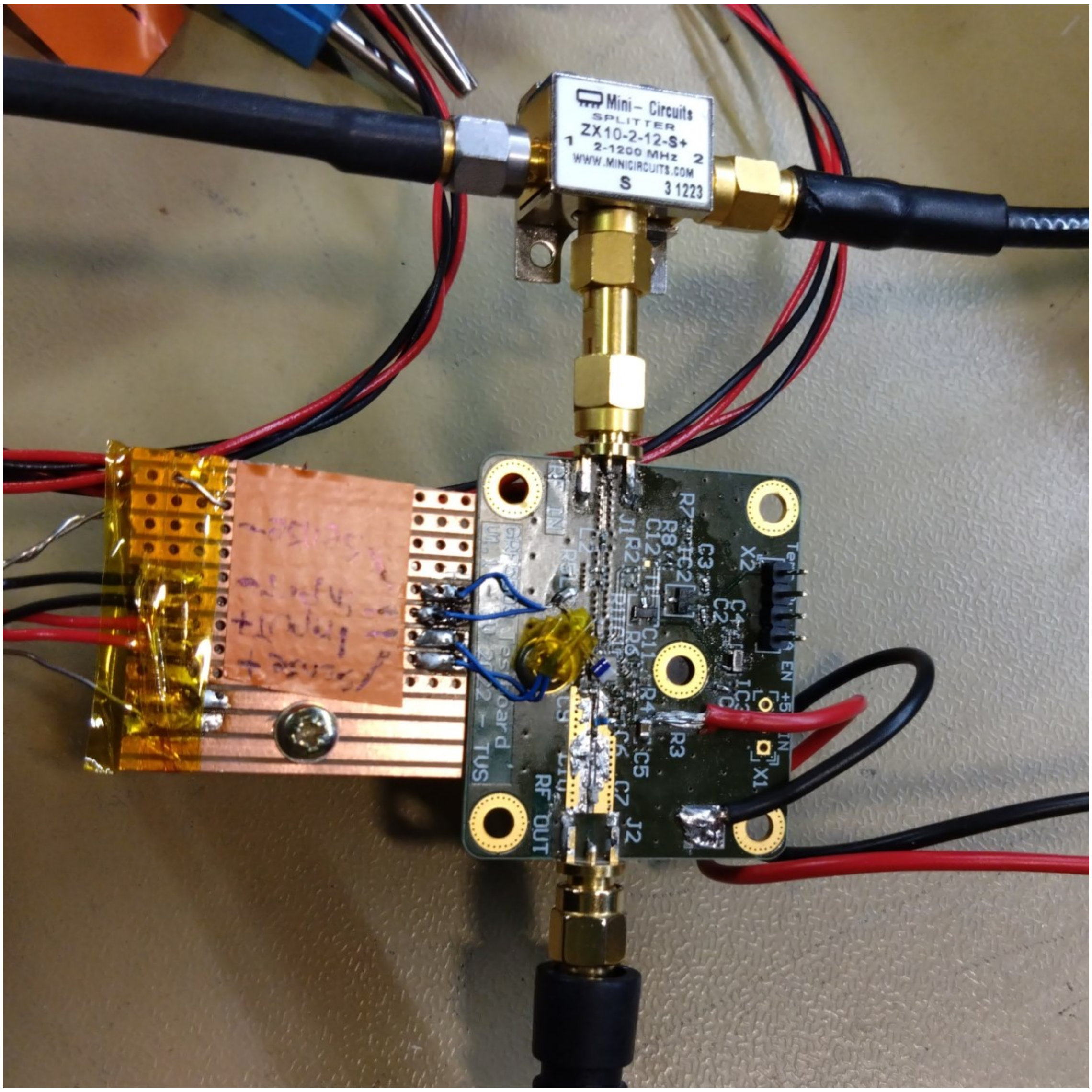

Figure 17. Mini-Circuits splitter connected to amplifier input.

Connecting the coupler directly to the amplifier board eliminates loss from a connecting cable and makes the measurement setup more compact.

7 Conclusions

The amplifier, as designed meets or exceeds most of the design requirements with a decent margin. Process and criteria for evaluating the suitability of RF amplifier solutions was successfully created and then used in evaluating this amplifier. As such both the process and amplifier solution ware found to be satisfactory.

References

1 GS1. EPC™ Radio-Frequency Identity Protocols Generation-2 UHF RFID Standard - Specification for RFID Air Interface Protocol for Communications at 860 MHz – 960 MHz [Internet]. 2018 Available from: https://www.gs1.org/sites/default/files/docs/epc/gs1-epc-gen2v2-uhf-airinterface_i21_r_2018-09-04.pdf (Accessed Apr 21, 2023).

2 FEIG. Model ID LR2500 HF Long range reader datasheet [Internet]. 2021. Available from: https://www.feig.de/fileadmin/user_upload/Downloads/Datenblaetter/Data_sheet_Identification_Stationary_Readers_ID_LR_M_2500.pdf (Accessed Apr 19, 2023).

3 ETSI. ETSI EN 302 208 V3.3.1 (2020-08) - Radio Frequency Identification Equipment operating in the band 865 MHz to 868 MHz with power levels up to 2 W and in the band 915 MHz to 921 MHz with power levels up to 4 W; Harmonised Standard for access to radio spectrum [Internet]. 2020 Available from: https://www.etsi.org/deliver/etsi_en/302200_302299/302208/03.03.01_60/en_302208v030301p.pdf (Accessed Apr 19, 2023).

4 FCC. 47 CFR Ch. 1, part 15. [Internet]. 2023. Available from: https://www.ecfr.gov/current/title-47/chapter-I/subchapter-A/part-15 (Accessed Apr 19, 2023).

5 Qorvo. RF5110G 150 - 960 MHz, 3 Volt General Purpose / Power Amplifier [Internet] (2023) Available from: https://www.qorvo.com/products/p/RF5110G (Accessed Apr 19, 2023).

6 Guerilla-RF. GRF5509 HIGH EFFICIENCY, 4-WATT PA 0.7 to 1 GHz [Internet]. https://www.guerrilla-rf.com/products/DataSheet?sku=5509&file_name=GRF5509DS.pdf (Accessed Apr 19, 2023).

7 Brandner PCB OÜ. Proprietary production quote provided to Turck Vilant Systems Oy by Brandner PCB OÜ. [2022]

8 Guerilla-RF. GRF5509 865-928 MHz: Linear Tune vs. High Power Tune [Internet] (2021) (Accessed Apr 19, 2023). Available from: https://www.guerrilla-rf.com/products/CustomTunes?sku=5509&file_name=GRF5509%20865-928%20MHz%20Linear%20Tune%20vs_%20High%20Power%20Tune.pdf (Accessed Apr 19, 2023).

9 Michael Margraf, QUCS Studio – A Free and Powerful Circuit Simulator, http://qucsstudio.de/ (Accessed Apr 19, 2023).

10 Panasonic. High Reliability Glass Epoxy Multi-layer Materials Laminate R-1755V [Internet]. (Jul 2019) Available from:

https://api.pim.na.industrial.panasonic.com/file_stream/main/fileversion/180183 (Accessed Apr 19, 2023).

11 Guerilla-RF. GRF5509 HIGH EFFICIENCY, 4-WATT PA [Internet]. (2023). Available from: https://www.guerrilla-rf.com/products/detail/sku/GRF5509#tabs-2 (Accessed Apr 19, 2023).

12 Texas Instruments. LM3480 100-mA, SOT-23, Quasi Low-Dropout Linear Voltage Regulator [Internet]. (Sept 2015) Available from: https://www.ti.com/lit/ds/symlink/lm3480.pdf?ts=1681909297501&ref_url=https%253A%252F%252Fwww.google.com%252F (Accessed Apr 19, 2023).

13 Onsemi. BSS84 - P-Channel Enhancement Mode Field-Effect Transistor [Internet]. (Oct 2021) Available from: https://www.onsemi.com/pdf/datasheet/bss84-d.pdf (Accessed Apr 19, 2023).

14 SIGLENT Technologies Co., Ltd. SSA3000X Spectrum Analyzer Data Sheet [Internet]. (2020) Available from: https://siglentna.com/wp-content/uploads/dlm_uploads/2017/10/SSA3000X_DataSheet_DS0703X_E05A.pdf (Accessed Apr 21, 2023).

15 TE Connectivity. PTF- FAMILY Platinum Temperature Sensors [Internet]. (2017) Available from: https://www.farnell.com/datasheets/2305684.pdf (Accessed Apr 19, 2023).

16 Fischer Elektronik. WLFT 404 datasheet. https://www.farnell.com/datasheets/50111.pdf (Accessed Apr 19, 2023).

17 NanoRFE. PC GUI software for NanoVNA V2 - PC GUI software for NanoVNA V2 [Internet]. (2022) Available from https://github.com/nanovna-v2/NanoVNA-QT (Accessed Apr 19, 2023).

18 Mini-Circuits. ZX10-2-12-S+ 2 - 1200 MHz splitter [Internet]. Available from: https://www.minicircuits.com/WebStore/dashboard.html?model=ZX10-2-12-S%2B (Accessed Apr 19, 2023).